Int. J. Electrochem. Sci., 6 **(2011)** 1230 - 1236

International Journal of
ELECTROCHEMICAL
SCIENCE
www.electrochemsci.org

Improvement of Photovoltaic Performance of Dye-Sensitized Solar Cell by Post Heat Treatment of Polymer-Capped Nano-Platinum Counterelectrode

Jo-Lin Lan[1], *Chi-Chao Wan*[1], *Tzu-Chien Wei*[2], *Wen-Chi Hsu*[2], *Chao Peng*[2], *Ya-Huei Chang*[2], *and Chih-Ming Chen*[3,*]

[1] Department of Chemical Engineering, National Tsing-Hua University, Hsin-Chu 300, Taiwan
[2] Hsin-Chu Laboratory, Tripod technology corporation, Hsin-chu 300, Taiwan
[3] Department of Chemical Engineering, National Chung Hsing University, Taichung 402, Taiwan
[*]E-mail: chencm@nchu.edu.tw

Received: 9 March 2011 / *Accepted:* 18 April 2011 / *Published:* 1 May 2011

A post heat treatment is developed to improve the "two-step dip coating process" in which poly-N-vinyl-2-pyrrolidone (PVP)-capped Pt nanoclusters are deposited with the aid of appropriate conditioner on transparent conductive oxide (TCO) glass as counterelectrode for dye-sensitized solar cell (DSSC). Charge transfer resistance (R_{CT}) is found only 0.56 Ω-cm^2 for this annealed counterelectrode. The improvement of R_{CT} is attributed to the removal of conditioner by the post heat treatment at 270 ^{o}C, which enhances the electrical contact between the Pt nanoclusters and the TCO glass, and thereby accelerates the charge transfer. The DSSC employing this annealed counterelectrode achieves a high energy conversion efficiency over 8%.

Keywords: Photovoltaic, Pt, annealing

1. INTRODUCTION

The dye-sensitized solar cell (DSSC) has undoubtedly caught world-wide attention due to its high energy conversion efficiency and potential to furnish low-cost solar electricity [1]. A typical DSSC consists of a dye-sensitized nanocrystalline TiO_2 film on transparent conductive oxide (TCO) glass as the photoanode, an electrolyte system containing iodide/tri-iodide (I^-/I_3^-) redox couple in a proper mediator, and a counterelectrode capable to catalyze the tri-iodide reduction. Although many materials show catalytic activity toward tri-iodide reduction [2-5], platinum (Pt) is still the most efficient one [5-10]. In addition, Pt-based catalysts are also widely used in other energy devices like fuel cells due to their superior catalytic performance [11-13]. Among various fabrication methods, sputtering is widely used to deposit a thin Pt layer on the TCO glass [6,7,9]. However, it requires high vacuum environment, which is expensive and apparently contradict to the claimed feature of low-cost DSSC. Considering future large scale production, it is necessary to develop a simple process to prepare Pt counterelectrode with low Pt loading and acceptable performance.

In our previous studies [14,15], we have successfully coated Pt nanoclusters protected by poly-N-vinyl-2-pyrrolidone (PVP) on TCO glass by a simple room temperature dip-coating process. The Pt-coated glass basically meets the abovementioned requirements and is potential as the counterelectrode for DSSC. Nevertheless, this counterelectrode still has room for improvement. For example, the conditioner used as a pre-treatment agent on the TCO surface might hinder the direct attachment of Pt nanoclusters with the TCO glass, and accordingly increases the internal resistance of DSSC. The PVP chains surrounding the Pt nanoclusters might hinder the direct contact of the Pt nanoclusters with the electrolyte, which results in a similar problem. In this study, we modify the existing dip-coating method by applying an additional post heat treatment. The post heat treatment enables efficient removal of the conditioner, and thereby the Pt nanoclusters can attach directly with the TCO glass which accelerates the electron transfer on the counterelectrode. A remarkable enhancement of the DSSC performance was achieved by employing the annealed Pt counterelectrode.

2. EXPERIMENTAL

The fluorine-doped tin oxide (FTO) glass (13 $\Omega\text{-}\square^{-1}$, 3.1 mm thick, Nippon Sheet Glass) was cleaned sequentially by 5% commercial glass cleaner (PK-LCG545, Parker) and deionized water. Cleaned FTO glass was immersed in a tank containing 1% conditioner (ML-371, OMGroup) at 60 ^{o}C for 5 min. The purpose of this step is to change the surface charge state for subsequent Pt deposition. The conditioned FTO glass was immersed in the PVP-capped Pt nanoclusters suspension for 5 min, in which the PVP-Pt suspension was prepared according to our previous studies [14,15]. Finally, the glass plate was rinsed with deionized water, dried in air, and heated to 60 ^{o}C to remove moisture. The Pt concentration was controlled at 1500 ppm. In this study, an additional post heat treatment was performed to remove the conditioner and/or PVP from the counterelectrode. The temperatures were set at 200, 270, and 500 ^{o}C and the time was 10 min. In order to understand the decomposition dynamics of PVP-capped Pt system, thermal gravimetric analysis (TGA) of the counterelectrodes with and without post heat treatment was conducted. For comparison, pure conditioner and PVP powder were also tested.

A symmetric cell was fabricated for electrochemical impedance spectroscopy (EIS) analysis which follows the concept comprising of two identical PVP-capped Pt counterelectrodes [15]. Ideally, three impedances including series resistance (R_S), charge transfer resistance (R_{CT}), and Nernst diffusion impedance (R_D) appear sequentially from high to low frequency in Nyquist plot according to EIS theory. In this study, we mainly focus on R_{CT} in the medium frequency range which represents the resistance pertaining to electrons transfer for the tri-iodide reduction on the Pt counterelectrode. In general, R_{CT} is used as an index to judge the catalytic performance of counterelectrode.

DSSC employing PVP-Pt counterelectrode was fabricated as follows. The nanocrystalline TiO_2 paste was made according to the published procedure [16] and scattering TiO_2 paste was purchased from CCIC (Catalysts & Chemical Ind. Co., Ltd.). A 15 μm-thick bi-layer TiO_2 film (12 μm nano-TiO_2+3 μm scattering-TiO_2) was coated on FTO glass by semi-automatic screen printer (ATMA, AT-45PA). The TiO_2/FTO photoanode was then immersed into titanium tetrachloride ($TiCl_4$) aqueous solution for post treatment. After preliminary drying at 120 ^{o}C for 5 min, the TiO_2 film was sintered sequentially in an oven at 325 ^{o}C for 5 min, 375 ^{o}C for 10 min, 450 ^{o}C for 10 min, and 500 ^{o}C for 10 min. Dye impregnation was done by immersing the sintered TiO_2 photoanode in 0.4 mM N719 (Everlight, Taiwan) Ru-based dye for 10 h. Dye-coated photoanode was then assembled with hole-drilled counterelectrode by pressing a hot melt film (Surlyn, 30 μm thick) in between at 110 ^{o}C for 20 s. Electrolyte (1M 1-propyl-2,3-dimethylimidazolium iodide (DMPII), 0.15M I_2, 0.5M 4-tert-butylpyridine (TBP), and 0.1M GuSCN in methoxypropionitrile (MPN)) was injected via hole to fill the cell. Photocurrent-voltage (I-V) curve was measured by a computer-controlled digital source meter (Keithley, model 2400) under AM1.5, 1 sun irradiation (Yamashita Denso, YSS150A-classA).

3. RESULTS AND DISCUSSION

Figure 1 is the Nyquist plot of symmetric cells comprising of two identical PVP-capped Pt electrodes with and without post heat treatment.

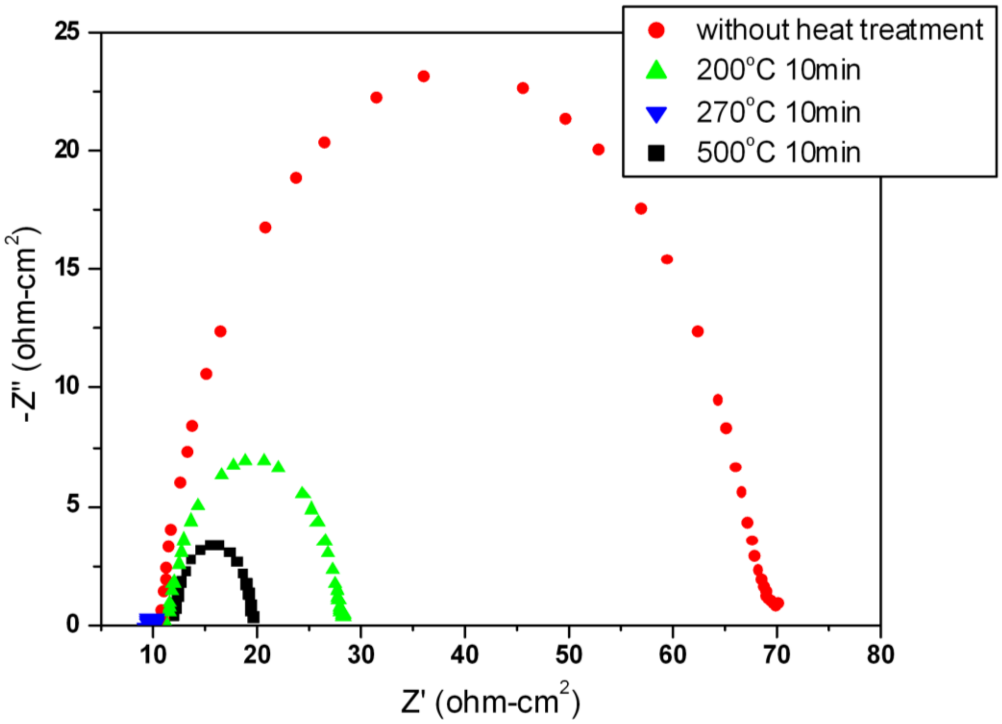

Figure 1. The Nyquist plot of the symmetric cells assembled by two identical Pt electrodes with and without post heat treatments.

The R_{CT} listed in Table 1 was determined by measuring the half of the diameter of the semi-circle. The R_{CT} of other Pt-based counterelectrodes previously published was also summarized in Table 1 for comparison. The PVP-capped Pt electrode via room temperature process (without post heat treatment) possessed a R_{CT} of 29.26 Ω-cm^2, which is one order of magnitude larger than that by thermally deposited Pt electrode (<1 Ω-cm^2) under similar test condition [2].

Table 1. The charge transfer resistances (R_{CT}) of the Pt-based counterelectrodes fabricated by various methods.

Pt-based counterelectrodes	Pt loading (μg-cm^{-2})	R_{CT} (Ω-cm^2)
PVP-capped Pt (Without heat treatment)	<5	29.26
PVP-capped Pt (10 min of heat treatment at 200 °C)	<5	8.4
PVP-capped Pt (10 min of heat treatment at 270 °C)	<5	0.56
PVP-capped Pt (10 min of heat treatment at 500 °C)	<5	3.87
Thermally deposited Pt [2]	5	<1
Screen-printed Pt [17]	20	5-10
Sputtered Pt [9]	1.4 nm (thickness)	0.45

However, the R_{CT} decreased drastically to 8.4, 0.56, and 3.87 Ω-cm^2 after post heat treatment at 200 °C, 270 °C, and 500 °C, respectively. It is suggested that the post heat treatment might remove part of PVP and conditioner, so that the Pt nanoclusters could be in contact with the electrolyte and the FTO substrate at a higher extent. The electron transfer on the Pt electrode became more efficient, and accordingly the R_{CT} reduced.

In order to clarify the effect of post heat treatment, the TGA results shown in Figure 2 are analyzed. It is found that the conditioner (curve A) decomposed around 200 °C, while PVP polymer (curve B) could remain relatively stable over 400 °C. Similar result was observed in the thermal behavior of PVP-capped Pt + conditioner without post heat treatment (curve C), where the conditioner burned out at 200~300 °C and then PVP decomposed partially until 500 °C. When the conditioned PVP-capped Pt was heated at 270 °C for 10 min before TGA test, the curve D shows that the weight loss is nearly zero before 300 °C, indicating that most conditioner has already been removed by heat treatment. After 300 °C, PVP gradually decomposed. Consequently, with the help of post heat treatment at 270 °C for 10 min, the conditioner can be removed efficiently while the PVP polymer still covers the Pt nanoclusters.

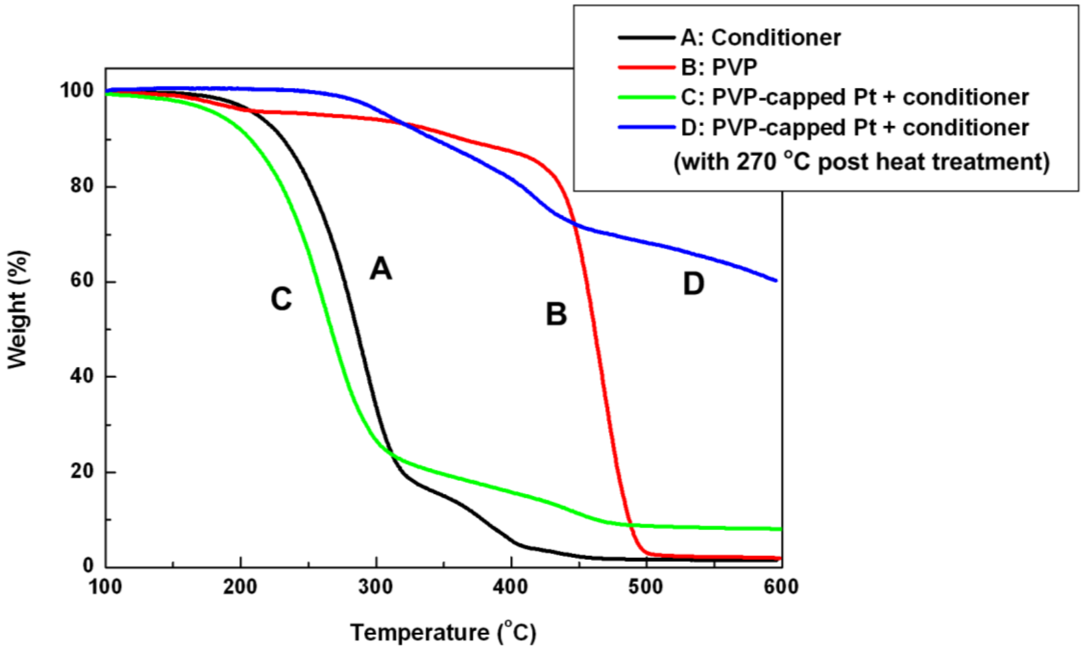

Figure 2. The thermal gravimetric analysis (TGA) of the PVP-capped Pt systems.

According to the above TGA results, the conditioner started to decompose at 200 °C. It indicates that the post heat treatment at 200 °C could remove part of the conditioner and thereby enhance the electrical contact between the PVP-capped Pt nanoclusters and FTO glass. Therefore, the R_{CT} reduced from 29.26 (without heat treatment) to 8.4 Ω-cm^2. When heating temperature was raised to 270 °C, the conditioner layer was almost burned out in 10 min and the remaining PVP-capped Pt nanoclusters were deposited on FTO glass without any intermediate layer.

The direct attachment of the PVP-capped Pt nanoclusters with the FTO glass enabled more efficient electron transfer and accordingly the R_{CT} was further reduced to only 0.56 Ω-cm^2. However, it is interesting to find that after 500 °C high temperature treatment, the R_{CT} (3.87 Ω-cm^2) was worse than that after 270 °C heat treatment. The TGA results suggest that the protecting polymer, PVP would decompose when the temperature exceeded 450 °C. The Pt nanoclusters may aggregate without the protective PVP outer layer, and instead the R_{CT} increased slightly due to the net decrease of active surface area of Pt. In summary, the removal of conditioner is beneficial for the electron transfer because of enhanced electrical contact between the PVP-capped Pt nanoclusters and FTO substrate, but the removal of the PVP capped layer led to the decrease of active surface area of Pt due to the Pt aggregation. Therefore, based on the variation of R_{CT} with the heating temperature, the optimal temperature of heat treatment was 270 °C.

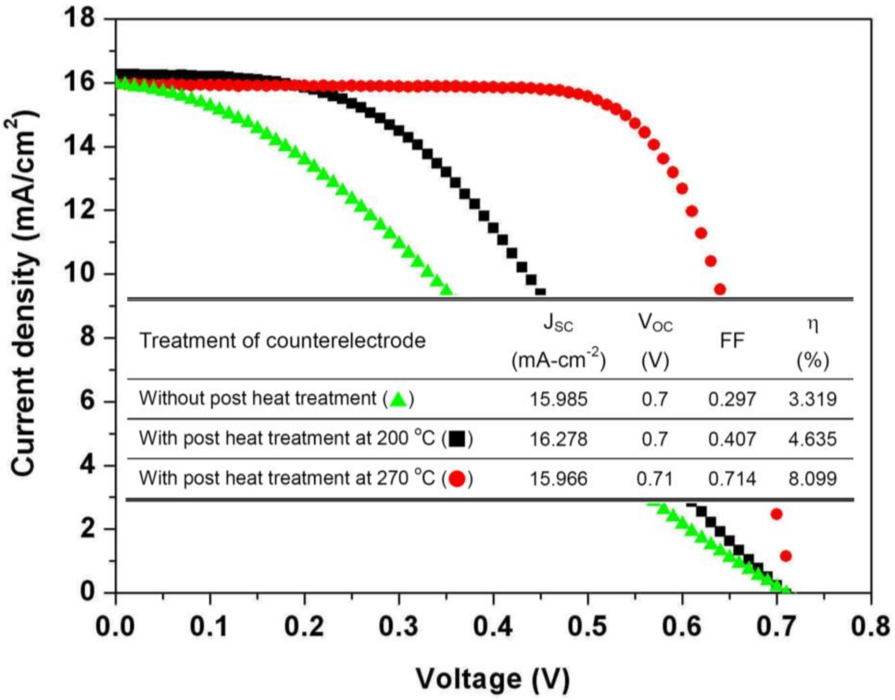

Treatment of counterelectrode	J_{SC} (mA-cm^{-2})	V_{OC} (V)	FF	η (%)
Without post heat treatment (▲)	15.985	0.7	0.297	3.319
With post heat treatment at 200 °C (■)	16.278	0.7	0.407	4.635
With post heat treatment at 270 °C (●)	15.966	0.71	0.714	8.099

Figure 3. The J-V curves of DSSCs fabricated by the PVP-capped Pt counterelectrodes with and without post heat treatment as well as the corresponding photovoltaic parameters.

DSSCs employing the PVP-capped Pt counterelectrodes with and without post heat treatment were tested under AM1.5 irradiation. The J-V curves are shown in Figure 3 as well as the corresponding photovoltaic parameters. The data with post heat treatment at 500 °C was not shown due to its increased R_{CT}. The DSSCs employing the counterelectrodes with post heat treatment exhibited higher energy conversion efficiencies (η) in comparison with that employing the counterelectrode without post heat treatment. The enhanced efficiency was mainly attributed to the improved fill factor (FF). In general, FF is an index which can reflect the internal resistance of cell. As discussed above, the post heat treatment can remove the conditioner and enhance the electrical contact between the Pt nanoclusters and the FTO substrate. The internal resistance of cell is reduced and therefore FF is enhanced. With post heat treatment at 270 °C, the conditioner was nearly burned out and accordingly FF achieved a remarkably higher value (0.714) as well as the efficiency (8.099%).

4. CONCLUSIONS

The existing “two-step dip coating” method for preparing a counterelectrode deposited with conditioned, PVP-capped Pt nanoclusters for DSSC has advantages of extremely low Pt loading (< 5 μg-cm^{-2}) and acceptable charge transfer resistance (29.26 Ω-cm^2) for electrocatalysis. With an additional post heat treatment at 270 °C for 10 min, remarkable enhancement can be achieved in the electrocatalytic performance due to the reduction of charge transfer resistance (0.56 Ω-cm^2). The TGA results indicate that the conditioner, which is used as a pre-treatment agent, can be removed efficiently by the post heat treatment at 270 ^{o}C. Without the conditioner, the Pt nanoclusters attach directly with the TCO glass and the charge transfer becomes more efficient due to reduced charge transfer resistance. The DSSCs employing the Pt counterelectrode with post heat treatment shows high energy conversion efficiency of 8.099 %, which is much better than that employing the Pt counterelectrode without post heat treatment (3.319 %).

ACKNOWLEDGEMENTS

The authors thank the financial support of the Ministry of Economic Affairs, Taiwan, R.O.C.

References

1. B. O’Regan, M. Grätzel, *Nature* 335 (1991) 737-740.
2. N. Papageorgiou, W.F. Maier, M. Grätzel, *J. Electrochem. Soc.* 144 (1997) 876-884.
3. T.N. Murakami, S. Ito, Q. Wang, M.K. Nazeeruddin, T. Bessho, I. Cesar, P. Liska, R. Humphry-Baker, P. Comte, P. Péchy, and M. Grätzel, *J. Electrochem. Soc.* 153 (2006) a2255-a2261.
4. Y. Saito, W. Kubo, T. Kitamura, Y. Wada, S. Yanagida, *J. Photochem. Photobiol. A* 164 (2004) 153-157.
5. T.N. Murakami, M. Grätzel, *Inorg. Chim. Acta* 361 (2008) 572-580.
6. X. Fang, T. Ma, G. Guan, M. Akiyama, T. Kida, E. Abe, *J. Electroanal. Chem.* 570 (2004) 257-263.
7. X. Fang, T. Ma, M. Akiyama, G. Guan, S. Tsunematsu, E. Abe, *Thin Solid Films* 472 (2005) 242-245.
8. C.M. Chen, C.H. Chen, T.C. Wei, *Electrochim. Acta* 55 (2010) 1687-1695.
9. Y.L. Lee, C.L. Chen, L.W. Chong, C.H. Chen, Y.F. Liu, C.F. Chi, *Electrochem. Commun.* 12 (2010) 1662-1665.
10. C.M. Chen, C.H. Chen, S.J. Cherng, T.C. Wei, *Mater. Chem. Phys.* 124 (2010) 173-178.
11. B. Krishnamurthy, S. Deepalochani, *Int. J. Electrochem. Sci*., 4 (2009) 386-395
12. J. Parrondo, R. Santhanam, F. Mijangos, B. Rambabu, *Int. J. Electrochem. Sci*., 5 (2010) 1342-1354
13. X.J. Feng, Y.L. Shi, Z.A. Hu, *Int. J. Electrochem. Sci*., 5 (2010) 489-500
14. T.C. Wei, C.C. Wan, Y.Y. Wang, *Appl. Phys. Lett.* 88 (2006) 103122.
15. T.C. Wei, C.C. Wan, Y.Y. Wang, C.M. Chen, H.S. Shiu, *J. Phys. Chem. C* 111 (2007) 4847-4853.
16. S. Ito, T.N. Murakami, P. Comte, P. Liska, C. Grätzel, M.K. Nazeeruddin, M. Grätzel, *Thin Solid Films* 516 (2008) 4613-4619.
17. N. Papageorgiou, *Coord. Chem. Rev*. 248 (2004) 1421-1446.